

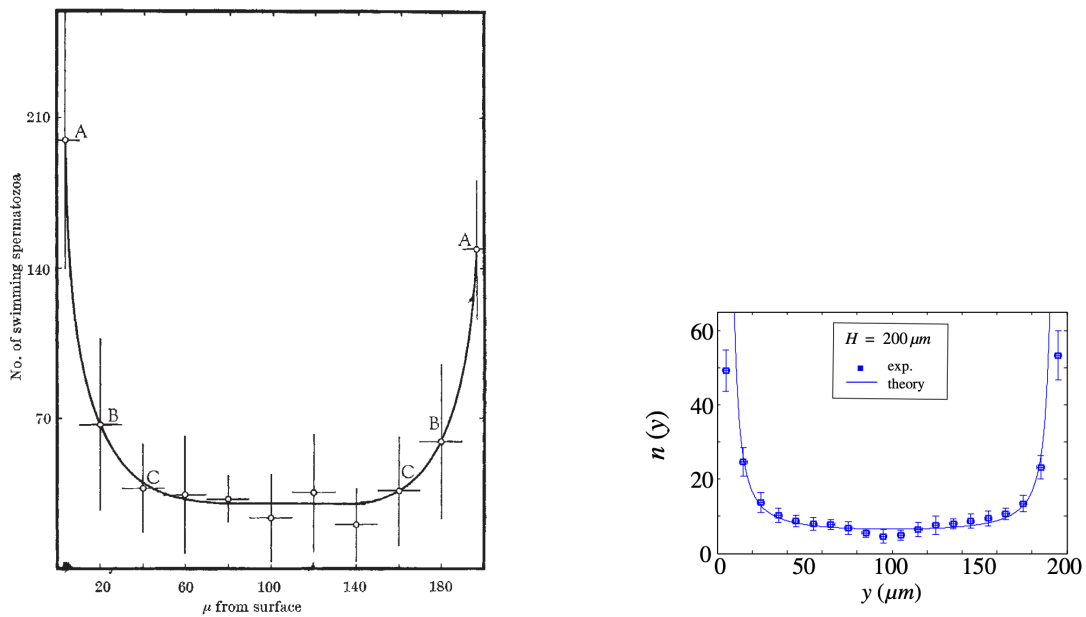
Brownian Microswimmers: Investigating models  
that capture boundary accumulation of  
microorganisms

Inti-Raymi Carhuancho Mantripp

Candidate Number: 1090497

# 1 Introduction

Many types of self-propelled microorganisms moving through water tend to accumulate near the boundaries of their environments. This has been observed both experimentally, [1], [2] and in nature. Figure 1 shows two characteristic illustrations of this behaviour by plotting the density cells and bacteria observed cross-sectionally within their domains.



(a) Distribution of bull spermatozoa in suspended medium [1].

(b) Distribution of E. coli bacteria between two glass plate [2].

Figure 1: Experimental results illustrating boundary accumulation of swimming microorganisms.

Many models have been proposed to describe the behaviour of microswimmers([3], [2], [4]), and this observed boundary accumulation is an important feature for such models to capture. The purpose of such models is not only to describe this behaviour but also to provide some explanation behind it.

The goal of this report is to present three models that describe the behaviour of swimming microorganisms, with a particular focus on capturing the observed boundary accumulation. Before introducing these models, a brief overview of stochastic PDEs and the Fokker-Planck equation will be given.

The structure of this report is as follows:

## 2 Main

The dynamics of microorganisms are in part the result of microscopic interactions between organisms and their surrounding environment SOURCE NEEDED. Rather than model this directly, this is typically captured by introducing stochastic terms to their dynamics. This is done in all the models covered in this report, and for that reason we will give an overview of stochastic differential equations (SDEs) followed by their solution via the Monte Carlo methods and the Fokker-Planck equation.

### 2.1 Stochastic Differential Equations and the Fokker-Planck Equation

For the purposes of this report, SDEs can be conceptually viewed as differential equations with an additional random term that introduces stochastic fluctuations to their dynamics.

To illustrate, consider the deterministic differential equation:

$$dx = \mu(x(t), t)dt.$$

Here,  $x(t)$  is a deterministic variable with a drift term  $\mu(x(t), t)$ , mapping  $\mathbb{R} \times [0, \infty) \rightarrow \mathbb{R}$ . By adding stochasticity through Brownian motion

$$dX = \mu(X(t), t)dt + \sigma(X(t), t)dW \quad (1)$$

where  $X(t)$  is now a stochastic process. Here,  $\mu(X(t), t)dt$  continues to be the deterministic drift term, while  $\sigma(X_t, t)$  is known as the *diffusion term*, scaling the stochastic fluctuations introduced by the Wiener process  $W_t$ . The increments of  $W_t$  are normally distributed as follows:

$$dW \sim \mathcal{N}(0, dt).$$

By selecting a sufficiently small time step  $\Delta t$ , we discretise equation (1) to numerically approximate the differential as:

$$\Delta X = \mu(X(t), t)\Delta t + \sigma(X(t), t)\Delta W \quad (2)$$

Equation (2) can be used in an iterative approach to obtain a sample trajectory of the SDE in equation (1):

$$X(t + \Delta t) = X(t) + \Delta X. \quad (3)$$

This method is called the Euler-Maruyama method, a stochastic analogue of the forward Euler method [5].

As  $X(t)$  is a stochastic process, at any fixed time  $t$ ,  $X(t)$  has a distribution described by its probability distribution function (PDF). To obtain the PDF of the random variable  $X(t)$  at a given time  $t$ , two main approaches exist. Firstly, using the Euler-Maruyama method one can generate  $n$  independent trajectories of the SDE. Provided  $n$  is sufficiently large, one can construct an empirical density from the realisations of  $X(t)$  at time  $t$ . This approach is called the Monte Carlo method, and its accuracy depends on the number of samples  $n$ . By the central limit theorem, the error in estimating the PDF decreases like:

$$\text{Error} \sim \mathcal{O}(n^{-1/2}).$$

This means that to halve the error we must quadruple the number of samples. This can make Monte Carlo methods computationally expensive for high precision estimates.

An alternative approach to determining the PDF is through the Fokker-Planck equation. The Fokker-Planck equatino is a partial differential equation (PDE) describing the evolution of the PDF  $p(x, t)$  associated with  $X(t)$ . For the SDE given in equation (1), the corresponding Fokker-Planck equation is:

$$\frac{\partial p(x, t)}{\partial t} = -\frac{\partial}{\partial x} [\mu(x, t)p(x, t)] + \frac{1}{2} \frac{\partial^2}{\partial x^2} [\sigma^2(x, t)p(x, t)], \quad (4)$$

where  $p(x, t)$  is the probability density function of the random variable  $X_t$ . Solving this PDE can directly yield the PDF without the sampling noise inherent in Monte Carlo simulations.

For systems involving multiple interacting stochastic processes, we consider a system of coupled SDEs:

$$d\mathbf{X}_t = \boldsymbol{\mu}(\mathbf{X}_t, t), dt + \boldsymbol{\Sigma}(\mathbf{X}_t, t), d\mathbf{W}_t, \quad (5)$$

where  $\mathbf{X}_t \in \mathbb{R}^n$  is a vector-valued stochastic process,  $\boldsymbol{\mu}(\mathbf{X}_t, t)$  is a vector of drift terms,  $\boldsymbol{\Sigma}(\mathbf{X}_t, t)$  is a diffusion matrix, and  $\mathbf{W}_t \in \mathbb{R}^m$  is a vector of independent Wiener processes. The associated Fokker-Planck equation describing the evolution of the joint probability density  $p(\mathbf{x}, t)$  for the system is given by:

$$\frac{\partial p(\mathbf{x}, t)}{\partial t} = -\nabla_{\mathbf{x}} \cdot [\boldsymbol{\mu}(\mathbf{x}, t)p(\mathbf{x}, t)] + \frac{1}{2}\nabla_{\mathbf{x}} \cdot (\nabla_{\mathbf{x}} \cdot [\boldsymbol{\Sigma}(\mathbf{x}, t)\boldsymbol{\Sigma}(\mathbf{x}, t)^T p(\mathbf{x}, t)]) . \quad (6)$$

where  $\nabla_{\mathbf{x}}$  is the gradient operator with respect to the spatial variables  $\mathbf{x}$ . Solving this PDE provides a direct method for obtaining the joint probability distributions of systems of interacting stochastic systems.

## 2.2 Model 1: Pure Stochastic Model

The first model we present considers an elliptic cell with orientation  $\theta$  placed within a channel of infinite width and fixed height  $H$ . The setup for this model is illustrated in Figure 2.

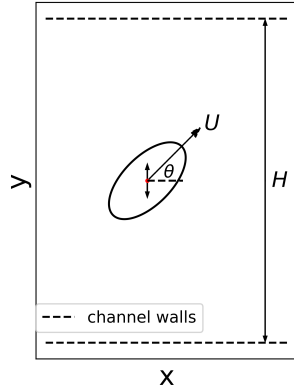


Figure 2: An elliptic cell with orientation  $\theta$  located within a channel of fixed height  $H$  and infinite width. The channel walls are considered reflective boundaries.

The dynamics imposed on the cell are described by the following coupled SDEs:

$$Y(t + \Delta t) = Y(t) + U \sin(\theta) + \sqrt{2D_y} \Delta W_1 \quad (7a)$$

$$\theta(t + \Delta t) = \theta(t) + \sqrt{2D_\theta} \Delta W_2 \quad (7b)$$

Here,  $Y(t)$  denotes the vertical position of the cell's geometric centre at time  $t$ , and  $\theta$  its orientation at that time. The parameters  $D_y$  and  $D_\theta$  scale the respective Brownian motion terms, modelling random fluctuations in position and orientation. The parameter  $U$  sets the deterministic speed of the cell's motion along the  $y$ -axis, thereby controlling the magnitude of the directed movement within the channel. We treat the upper and lower channel walls as reflective boundaries. Movement along

the  $x$ -axis is disregarded, as our primary interest is in understanding whether this system exhibits boundary accumulation behaviour. Given the channel's infinite extent along the  $x$ -axis, horizontal movements have no meaningful impact on the boundary accumulation analysis. care primarily about whether this system exhibits boundary accumulating behaviour. With no bounds along  $x$ , it is irrelevant to consider movement along the  $x$ -axis.

Our primary objective is to identify whether this system exhibits boundary accumulation behaviour. To investigate this, we seek the stationary distribution - the long-term PDF to which the system converges as  $t \rightarrow \infty$ . To obtain this stationary distribution, two approaches are available: Performing Monte Carlo simulations using equations (7), or directly solving the corresponding Fokker-Planck PDE.

Both of these approaches however first require us to identify the configuration space of the system - the space of possible configurations of  $y$  and  $\theta$  the system can inhabit. As the cell's orientation  $\theta$  is periodic and thus unbounded, the vertical position  $y$  is constrained by the channel walls. Specifically, the minimum distance the centre of the clel can approach each channel wall depends explicitly on its orientation  $\theta$ . This dependency is illustrated in Figure 3.

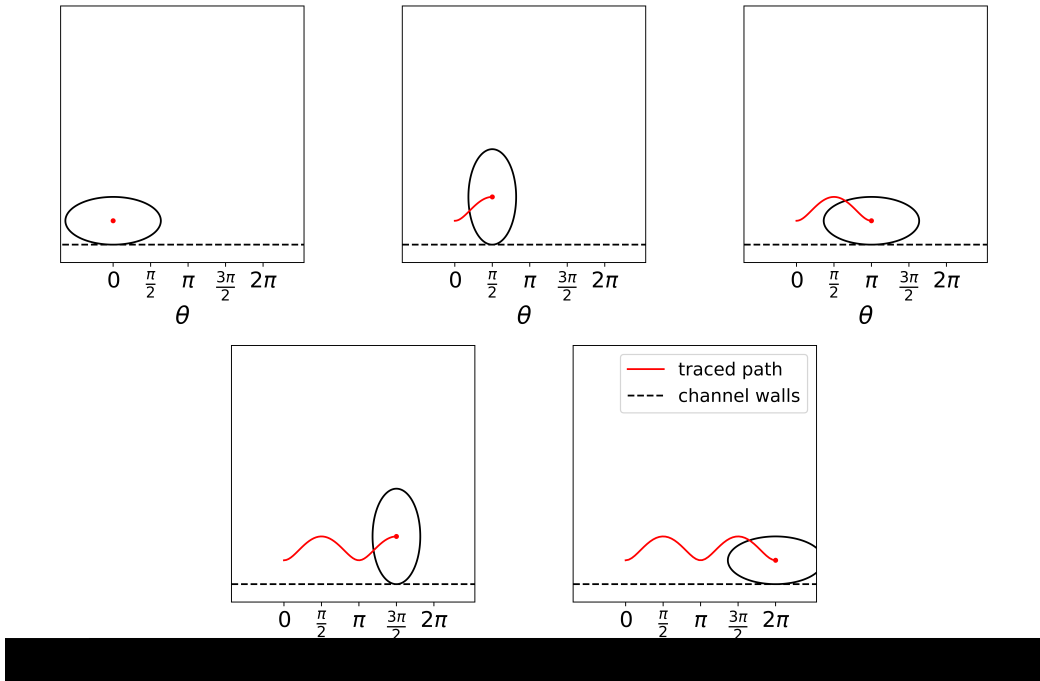


Figure 3: Path traced by the oval's centre, illustrating the minimum distance achievable to a horizontal wall as a function of orientation  $\theta$

The function characterising this minimum distance is termed the *wall distance*

function [3]. For the specific case of an ellipse, this function is defined by:

$$y_{min}(\theta) = \sqrt{a^2 \sin^2(\theta) + b^2 \cos^2(\theta)} \quad (8a)$$

$$y_{max}(\theta) = H - \sqrt{a^2 \sin^2(\theta) + b^2 \cos^2(\theta)} \quad (8b)$$

where  $a$  and  $b$  are the major and minor semi-axes for the elliptic cell, respectively. Equations (8) establish the upper and lower boundaries of the configuration space for this system. Figure 4 illustrates the derived configuration space.

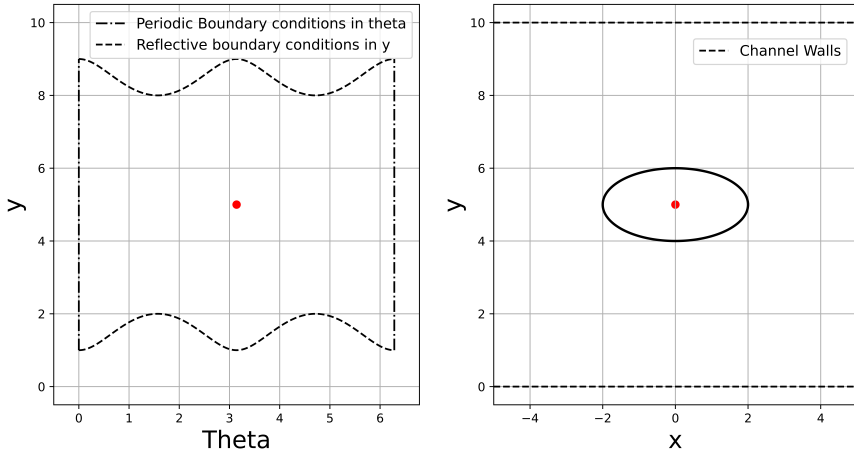


Figure 4: Configuration space for Model 1 and its correspondance to the physical system of a cell within a channel. Parameters used:  $a = 2$ ,  $b = 1$ ,  $H = 10$

Figure 4 also shows the boundary conditions applied to the configuration space. Periodic boundary conditions on the orientation variable  $\theta$  at  $\theta = 0$  and  $\theta = 2\pi$ , while reflective boundary conditions are applied at the upper and lower boundaries described by  $y_{min}(x)$  and  $y_{max}(x)$ .

With a clearly bounded configuration space, the corresponding Fokker-Planck equation associated with equations (7) can be solved. The corresponding Fokker-Planck equation is:

$$\frac{\partial p}{\partial t} = -\frac{\partial}{\partial y}(U \sin(\theta)p) + D_\theta \frac{\partial^2 p}{\partial \theta^2} + D_y \frac{\partial^2 p}{\partial y^2} \quad (9)$$

When solving equation (9), no-flux boundary conditions are applied at the upper and lower boundaries along the  $y$ -axis, accounting for the conservation of probability within the domain. The finite element solver COMSOL Multiphysics® was used to

numerically obtain the stationary distribution [6]. The resulting PDF is presented in Figure 5a, and the resulting marginal distribution across the channel is displayed in Figure 5b.

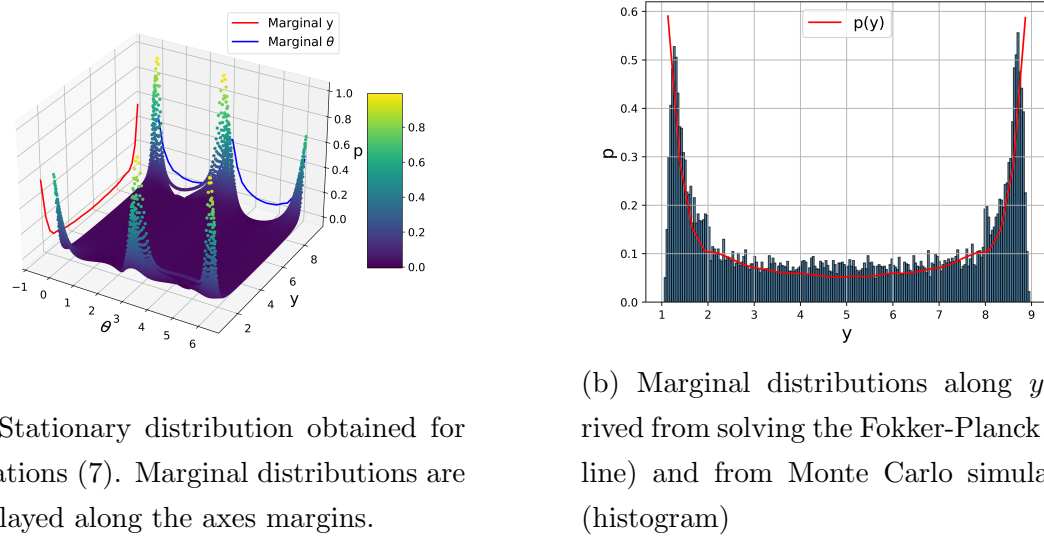


Figure 5: Comparison of stationary distribution and its marginal along  $y$ .

The marginal distribution along the  $y$ -axis clearly exhibits characteristic boundary accumulation behaviour. We attribute this phenomenon as arising from two primary mechanisms. Firstly, the drift term in equation (7a) implies that, on average, the cell moves towards and eventually encounters the boundary, where it becomes constrained until it sufficiently reorients. Secondly, the geometry of the configuration space contributes significantly; the elliptical shape introduces two "hills" with reflective boundaries. These features act as barriers, hindering the ease with which the system can exit the boundary regions, thus enhancing the boundary accumulation.

### 2.3 Model 2: Hydrodynamics Informed Model

The second model investigated was proposed by Chen *et al.* [3], building on the work of Spagnolie *et al.* [7]. This advances on the previous model by incorporating hydrodynamic interactions with the channel walls into the SDEs for the cell.

Spagnolie *et al.* approximate the velocity field around an elliptic swimmer by first treating the system as a *stresslet* - a force dipole - and then by Faxén's Law obtaining the corresponding velocity field for a swimmer with elliptic shape. Figure shows two illustrative charts of a microswimmer treated as a stresslet, and the velocity field

around this elliptic stresslet near the boundary.

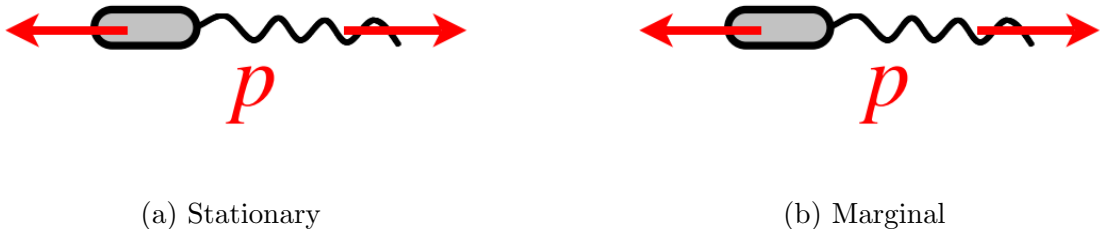


Figure 6: Comparison of stationary distribution and its marginal along  $y$ .

## References

- [1] Rothschild. “Non-random distribution of bull spermatozoa in a drop of sperm suspension”. In: *Nature* 198.4886 (1963), pp. 1221–1222.
- [2] Allison P Berke et al. “Hydrodynamic attraction of swimming microorganisms by surfaces”. In: *Physical Review Letters* 101.3 (2008), p. 038102.
- [3] Hongfei Chen and Jean-Luc Thiffeault. “Shape matters: a Brownian microswimmer in a channel”. In: *Journal of Fluid Mechanics* 916 (2021), A15.
- [4] Bao-quan Ai et al. “Rectification and diffusion of self-propelled particles in a two-dimensional corrugated channel”. In: *Physical Review E* 88.6 (2013), p. 062129.
- [5] Radek Erban and S Jonathan Chapman. *Stochastic modelling of reaction-diffusion processes*. Vol. 60. Cambridge University Press, 2020.
- [6] COMSOL AB. *COMSOL Multiphysics® v6.3*. Available: <https://www.comsol.com>. Stockholm, Sweden, 2024.
- [7] Saverio E Spagnolie et al. “Geometric capture and escape of a microswimmer colliding with an obstacle”. In: *Soft Matter* 11.17 (2015), pp. 3396–3411.